Available online at www.sciencedirect.com
ScienceDirect
Optics Communications 273 (2007) 500–505
OPTICS COMMUNICATIONS
www.elsevier.com/locate/optcom

Optimized performance map of an EAM for pulse generation and demultiplexing via FROG characterization

R. Maher *, P.M. Anandarajah, L.P. Barry

Research Institute for Network and Communications Engineering, School of Electronic Engineering, Dublin City University, Dublin 9, Ireland

Received 27 October 2006; received in revised form 3 January 2007; accepted 15 January 2007

Abstract

We demonstrate the complete characterization of a sinusoidally driven electro-absorption modulator (EAM) over a range of RF drive voltages and reverse bias conditions. An accurate performance map for the EAM, to be employed as a pulse generator and demultiplexer in an optical time division multiplexed (OTDM) system, can be realized by employing the Frequency Resolved Optical Gating technique. The generated pulses were characterized for chirp, extinction ratio (ER) and pulse width (<4 ps). The optimization of the EAM's drive conditions is important to ensure that the generated pulses have the required spectral and temporal characteristics to be used in high-speed systems. The ER and pulse width also influence the demultiplexing performance of an EAM in an OTDM system. This is confirmed by utilizing the EAM as a demultiplexer in an 80 Gb/s OTDM system and measuring the BER as a function of the received optical power for various values of the ER and pulse width. It is of paramount importance to accurately characterize the performance of each individual EAM as the modulators characteristics are device dependant, thus optimum performance can be achieved with slight variations to the device's drive conditions. By employing FROG, an optimum performance map of each specific device can be deduced. Simulations carried out verified the experimental results achieved.

Keywords: Pulse generation; Demultiplexing; Electro-absorption modulator (EAM); FROG

1. Introduction

Optical time division multiplexing (OTDM) and hybrid wavelength division multiplexing (WDM)/OTDM are technologies that could be used for greatly increasing the capacity of optical communication systems without increasing the cost (by avoiding high-speed electronics). As optical systems move towards higher data rates and also migrate from non-return to zero (NRZ) to return to zero (RZ) format (due to enhanced performance of RZ systems at 40 Gb/s and beyond) [1], the impact of chromatic dispersion in transmission fiber becomes more dramatic and the use of dispersion management techniques and/or optical fiber non-linearities to counteract the dispersive effects, must be precisely regulated [2]. In addition to knowing the dispersion parameter of the transmission fiber, it is essential to know the chirp, pulse width and ER of the optical data signals generated at the transmitter of these high-speed systems. This is necessary since the chirp of the optical pulses determines the propagation of the optical data [3]; the pulse width limits the bandwidth capacity of the system and also contributes to inter-symbol interference [4]; and the ER limits the systems performance as a consequence of coherent interference noise between individual OTDM channels [5]. Hence, to optimize the overall performance of a high-speed photonic communication system, it is vital to characterize accurately the intensity, picosecond duration and phase of the optical RZ data signals generated at the transmitter. As standard measurement techniques will not suffice in yielding such information, an alternative technique known as Frequency Resolved Optical Gating (FROG) is employed for the accurate and complete characterization of the signals.

* Corresponding author. Tel.: +353 1 7005884; fax: +353 1 7005508.
E-mail address: robert.maher@eeng.dcu.ie (R. Maher).

0030-4018/$ - see front matter © 2007 Elsevier B.V. All rights reserved.
doi:10.1016/j.optcom.2007.01.046

Short optical pulses can be generated by employing several different techniques such as mode locking, gain switching or by gating Continuous Wave (CW) light with an Electro-Absorption Modulator (EAM). Mode locking of semiconductor or fiber lasers is a common technique used to generate short optical pulses operating at high frequencies. However, the cavity complexity and limited tunability of the mode locking repetition rate act as major disadvantages associated with this technique. Alternatively, gain-switching offers smaller footprint, efficient wavelength-stable performance and the ability to produce high-repetition rate pulses. Nevertheless this technique has a number of shortcomings such as the generated pulses exhibiting a large chirp, timing jitter and a degraded Side Mode Suppression Ratio (SMSR) [6]. A suitable technique to generate picosecond optical pulses that exhibit high spectral and temporal purity involves gating a CW light source with a sinusoidally driven EAM [7]. This technique has been demonstrated to be reliable and is a stable source of short optical pulses. Low drive voltage, high modulation efficiency and polarization insensitivity are other qualities that make the semiconductor based EAM very attractive for high-speed optical communication systems.

When considering OTDM systems it is equally important to have stable demultiplexing schemes in addition to having a suitable pulse source [8]. The use of EAMs for optical demultiplexing has been demonstrated at rates up to 160 Gb/s [9]. With this technique the switching window of the EAM for demultiplexing should have a narrow width (approximately 30% of the bit slot duration to avoid interference), high extinction ratio, small timing jitter and long term stability in order to ensure error free performance at the receiver [10,11].

In this work, we demonstrate a map which shows an optimized region (chirp, ER and width) of operation when the bias and RF drive voltages of an EAM are varied. Hence, by completely characterizing the pulses over a range of driving conditions, a performance map can be constructed which illustrates the optimum operating condition of the EAM not only as a pulse generator but also as a demultiplexer. The technique of frequency resolved optical gating is used to realize the accurate and complete characterization.

2. Accurate pulse characterization via frequency resolved optical gating

There are many different techniques that are available for measuring short optical pulses. However, as optical systems move towards data rates of 100 Gb/s and beyond on each wavelength channel, it becomes increasingly difficult to accurately characterize the optical data pulses. The main problem is that the optical pulse duration in these systems is typically less than 5 ps, making it impossible for high-speed detectors and oscilloscopes to monitor pulse shape. In addition to pulse shape, it is also necessary to accurately characterize the exact phase or frequency across the optical pulse. Standard autocorrelation techniques only provide information in terms of pulse width and extinction ratio; it provides no phase information and assumes the pulse shape. The latter information is vital since the propagation of the optical data is determined by the exact intensity and phase of the optical pulses from the transmitter, in conjunction with the dispersion and non-linearity of the transmission fiber. To optimize the overall performance of high-speed systems, it is vital to be able to characterize accurately the intensity and phase of the optical data signals generated at the transmitter, and also at various optical processing devices along the transmission line (e.g. regenerators, wavelength converters, demultiplexers).

The FROG technique retrieves the complete electric field of an optical pulse, thus providing pulse width, intensity, phase and chirp characteristics. Frequency resolved optical gating is based on the spectral resolution of the output from a non-collinear autocorrelator, as described in [12], to generate a spectrogram of the pulse from which the intensity and phase can be recovered. In our work we used a FROG measurement system that employs SHG in a $LiNbO_3$ crystal with an interaction length of 250 μm. The non-linear crystal was quasi-phase matched and the SHG signal was spectrally resolved using a grating spectrometer with a 1024 – element cooled photodiode array mounted on the output. The spectral resolution was $\Delta\lambda = 0.04$ nm at a SHG wavelength of 775 nm. The autocorrelator delay was controlled by a stepper motor with a temporal resolution of $\Delta\tau = 6.7$ fs. At each delay instant, the measured spectrum was averaged for 0.4 s.

A standard retrieval algorithm was used to determine the complete electric field of the measured spectrogram. It is important that any data used as an input to the FROG algorithm contains the entire trace and that there is zero signal intensity around the perimeter of the measured spectrogram. High levels of noise in the perimeter acts as non-zero intensity, thus reducing the accuracy of the algorithm retrieval [13], therefore, the background noise was subtracted. Significantly better algorithm performance can be achieved if the noise level is maintained at a minimum value. In our work, we obtained a good signal to noise ratio (SNR), and hence high sensitivity by employing a low noise EDFA before the FROG. Using our setup we have already demonstrated the ability of our FROG to measure the extinction ratio up to approximately 30 dB [14–17].

3. Pulse generation

The experimental setup we used for the DC transfer characterization and the subsequent pulse generation is illustrated in Fig. 1. The EAM was a commercially available fiber pigtailed InP modulator that operates over the entire C-band and has 10InGaAs wells with InAlAs barriers. The basic setup for static characterization consists of an external cavity laser (ECL) providing an output power of 6 dBm to the EAM. A power meter measures

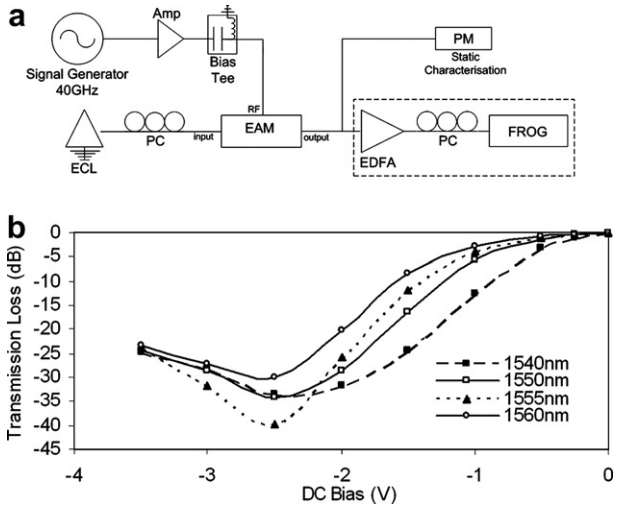

Fig. 1. (a) Experimental setup used for pulse generation and (b) DC transfer characteristic measured at a range of wavelengths.

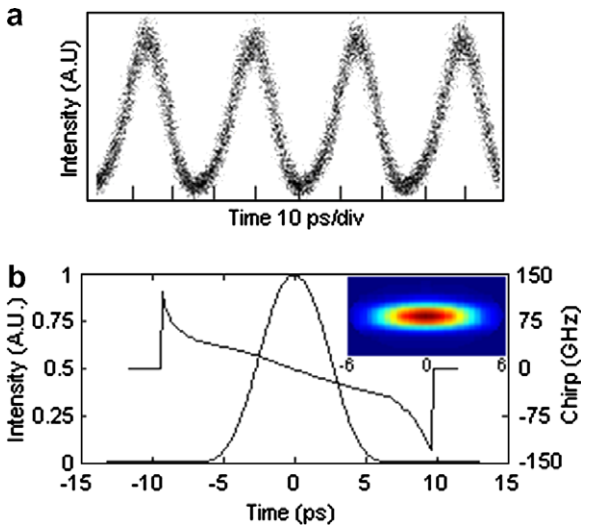

Fig. 2. Pulses generated using CW laser followed by an EAM, (a) characterized with 50 GHz oscilloscope and (b) pulse and corresponding chirp characterized using the FROG technique and inset, FROG spectrogram (center wavelength 775 nm).

the transmission loss as a function of reverse bias, thus illustrating the components variation in throughput with respect to a change in reverse bias voltage for a variety of wavelengths, and as a result this will have an impact on the optimum operating condition of the EAM for pulse generation and demultiplexing applications. This strong variation with respect to wavelength is due to the Quantum Confined Stark Effect (QCSE) in quantum well structures. The insertion loss shows little variation for different wavelengths, but the whole extinction curve and thus the optimum bias voltage experiences a large shift with respect to the emission wavelength.

The 40 GHz optical pulses were generated by gating CW light from an ECL by applying a sinusoidal wave of varying peak to peak amplitude in conjunction with a DC bias, via a bias tee, to the modulator. The bias voltage was then altered between 1 and 2 V in steps of 0.2 V and the pulses were analyzed at RF drive voltages of 2.5, 2.8, 3.1, 3.4 and 3.7 Vpp, respectively. The generated pulses were subsequently amplified to an average power of approximately 100 mW, with a specially designed short pulse erbium doped amplifier (EDFA) (as indicated in the dotted box, Fig. 1a) and characterized using the FROG technique as fully explained in Section 2. Pulse retrieval for the characterization carried out in this work routinely gave low retrieval errors of less than 0.0004 with 64×64 grid (i.e., 64 spectral and temporal points). In addition to the FROG measurement, the generated pulses were measured using an optical spectrum analyzer and a 50 GHz oscilloscope in conjunction with a 50 GHz detector.

The bias voltage and RF drive applied to the EAM were initially set to those values thought to generate optimum pulses from the setup, as deduced from the transfer characteristic (Fig. 1b). Fig. 2a displays the generated 40 GHz pulses measured with a 50 GHz oscilloscope in conjunction with a 50 GHz detector. Due to the limited response time of this detection system, it is difficult to obtain information about the characteristics of the generated pulses. In addition, as the bias voltage and RF drive signal applied to the EAM were varied, no noticeable changes were observed on the oscilloscope (not even pulse width). The pulses were subsequently characterized using the FROG technique.

Fig. 2b illustrates an example of the intensity and phase as measured using the FROG technique and also illustrates the raw data (spectrogram) for the retrieved pulse (inset Fig. 2b). The FROG technique enabled characterization of the EAM's performance in terms of pulse width, frequency chirp and extinction ratio (ER). By monitoring each of these parameters at various bias and drive conditions, an accurate performance map for the EAM could be deduced. Fig. 3 illustrates how the full width half maximum (FWHM) of the generated pulses, depends strongly on the reverse bias. As the reverse bias is increased, there is a noticeable decrease in pulse width. From these results, we can deduce that to achieve the narrowest width the EAM must be biased at 2 V with a large RF drive voltage.

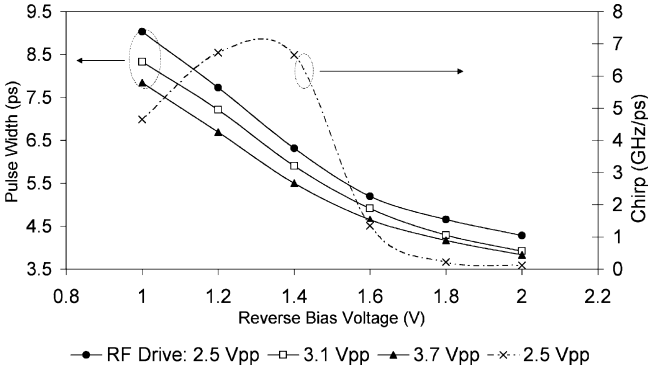

Fig. 3. Pulse width (FWHM) and frequency chirp as a function of reverse bias and RF drive voltage.

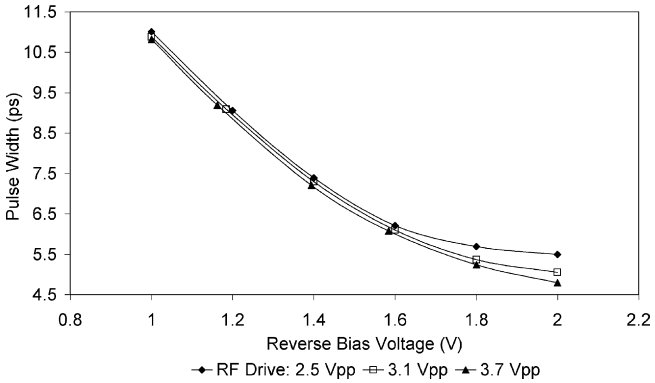

Fig. 4. Modeled Pulse Width as a function of reverse bias and RF drive voltage.

Similarly, the frequency chirp also depends strongly on the bias condition of the EAM. As the reverse bias increases there is a considerable decrease in frequency chirp (expressed in GHz/ps across the center of the pulse). The minimum chirp and thus near transform limited pulses (TBP = 0.43) can be achieved by biasing the EAM in the 1.6–2 V bias range. Thus, to achieve a short pulse with low chirp and high extinction it would be recommended to bias the modulator at 1.6 V with a large RF drive voltage. Using the FROG is an accurate way of characterizing EAM performance since the optimum operating condition is device dependant. To verify the pulse width versus bias voltage characteristic the CW experiment was simulated using the Virtual Photonics Incorporated software package. Fig. 4 illustrates the pulse width as a function of reverse bias for alternating drive voltages of 2.5, 3.1, and 3.7 Vpp. It can be seen that the trend of decreasing pulse width as a function of reverse bias is verified. There is also a decrease in pulse width relative to increasing RF drive, which also corresponds to the trend of the experimental results. There are slight discrepancies in the pulse width obtained from the model but this can be attributed to the differences between the static and dynamic response of the EAM. The simulation model is only concerned with the static characteristic and therefore does not compensate for the dynamic response of the EAM resulting is slightly larger pulse widths.

If there is a sufficient signal to noise ratio, the FROG can measure the extinction ratio of the pulse or gate up to approximately 30 dB [15]. The extinction ratio is an important pulse parameter, but it is also important to have good gate extinction when employing the EAM as a demultiplexer to ensure optimum BER performance. Therefore, this parameter is dealt with in more detail in the next section which is concerned with optimizing the EAM for demultiplexing.

4. High-speed demultiplexing

Fig. 5 illustrates the 80 Gb/s test bed used in this work to characterize the demultiplexing performance of a sinusoidally driven EAM. The transmitter consisted of a commercially available Tunable Mode Locked Laser (TMLL) which was optically amplified and filtered before it was modulated with a Pseudo-Random Bit Sequence (PRBS) of length $2^7 - 1$ with the aid of a Mach–Zehnder modulator. The PRBS was generated by a 10 Gb/s Pulse Pattern Generator (PPG). The resultant STM-64 RZ optical signal was multiplexed up to 80 Gb/s by passing it through a passive fiber interleaver. The polarization state of each tributary was maintained by placing a polarization controller at the input and a polarizer at the output of the multiplexer.

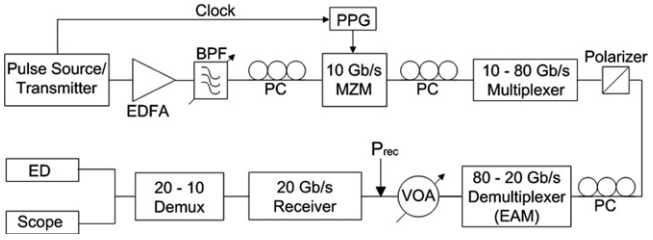

Fig. 5. 80 Gb/s test bed used to accurately measure the BER performance of an EAM operating as a 80–40 Gb/s demultiplexer.

The 80 Gb/s system was initially demultiplexed down to 40 Gb/s using the electro-absorption modulator. The bias and RF drive voltages applied to the EAM are consistent with the pulse generation experiment described in Section 3. This produced a varying gate width and ER which would have an effect on the optimum system demultiplexing performance. As before the system was analyzed for a range of reverse bias conditions and RF drive voltages. The optical data was demultiplexed down to 20 Gb/s with the aid of a Mach–Zehnder modulator (MZM) before it was optically pre-amplified and detected. Demultiplexing down to the base rate (10 Gb/s) was carried out with the aid of an electrical demultiplexer. BER measurements were performed for a range of received optical powers (measured before the 20 Gb/s receiver stage). Signal analysis was carried out with a 50 GHz oscilloscope in conjunction with a 50 GHz detector and the BER performance was monitored with an error detector.

The bias and RF driving conditions of the EAM were altered and a BER test was carried out for each permutation. Over the range of EAM operating conditions the duration of the switching window is narrow enough to correctly demultiplex from 80 to 40 Gb/s without introducing errors. It is therefore the ER of the gate combined with the varying signal to noise ratio (SNR), due to varying attenuation in the EAM; that is the primary cause of degraded performance. The magnitude of the ER changes due to the transmission profile of the EAM (Fig. 1b). Fig. 6 illustrates the ER ratio of the generated pulses (measured using FROG) when a drive voltage of 3.7 Vpp is applied the EAM at each bias point from 1 to 2 V, and it is seen to be at its peak at a bias voltage of 1.4 V. Beyond this bias point the ER drops off rapidly and this degradation in

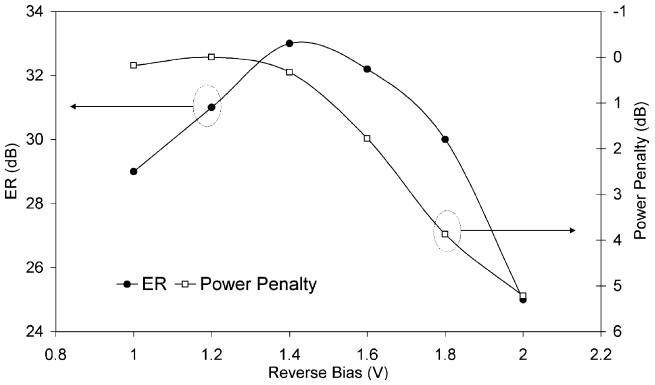

Fig. 6. Experimentally measured extinction ratio and BER performance at $1e^{-9}$ as a function of reverse bias.

ER with respect to the bias voltage may cause corresponding power penalties during the demultiplexing process. BER tests were performed at various EAM operating conditions and the result is plotted in terms of the power penalty at a bit error rate of $1e^{-9}$ (relative to the optimum performance) and the reverse bias condition of the EAM.

At a reverse bias of 1 V the extinction ratio is assumed large enough to produce error free performance. As the bias increases the ER also increases but this improvement is somewhat negated by a decrease in SNR as deduced from the transfer characteristic in Fig. 1b. Even though the optimum ER is realized at a bias point of 1.4 V there is a degraded SNR at this level than that at 1 or 1.2 V, due to a steeper gradient on the transmission curve. This results in a small power penalty with respect to 1.2 V. After this point the ER decreases and combined with a decreasing SNR a larger power penalty of up to 5.5 dB at a bias point of 2 V is experienced. The optimum bias condition for the EAM when employed as a high-speed demultiplexer varies to that when used for pulse generation. When considering pulse generation the critical parameters are pulse width and extinction ratio, although when considering demultiplexing the receiver sensitivity indicates the optimum performance of the device. As explained above, this receiver sensitivity is at its maximum when the EAM is operating in its low loss regime, thus providing a larger SNR combined with a high ER, resulting in good BER performance. For this reason the EAM should be biased at 1.2 V when employed as a demultiplexer and between 1.6 and 2 V when employed as a pulse generator.

5. Simulation model

To verify these experimental results, the 80 Gb/s OTDM system was modeled using the Virtual Photonics Incorporated (VPI) software package. Fig. 7 shows a schematic of the setup. The model initially creates a secant squared optical pulse with a FWHM of 2.1 ps at a repetition rate of 10 GHz to model that of the TMML in the experimental setup. The output of the pulse source is split into eight optical channels which are then individually modulated with a 10 Gb/s signal via eight amplitude modulators. Each tributary is time delayed before being optically multiplexed to form an 80 Gb/s OTDM data signal. The Virtual Photonics Incorporated software package provides a measured electro-absorption modulator (EA_measured). This module simulates an electro-absorption modulator with a voltage-dependant transmission function, phase shift and alpha factor, which are represented by eight order polynomials. The input signal $E(t)$ is analyzed within a specific time window, which suppresses $E(t)$ outside a certain region, defined by the form of the window. The number of samples is defined by the length of the time window divided by a downsampling factor. By specifying the transfer function of the EA device combined with the phase and alpha factor, an accurate simulation comparison can be achieved.

The EAM is used as an 80–40 Gb/s demultiplexing component. The 40 Gb/s data signal is optically amplified and then demulitplexed down to the base rate of 10 Gb/s using two Mach–Zehnder modulators. The receiver consists of a variable optical attenuator, photodetector and low pass filter. As in the experimental procedure, the reverse bias is altered between 1 and 2 V in steps of 0.2 V. The RF drive voltages were also altered correspondingly. BER tests were performed at the various EAM operating conditions and the result is plotted in terms of the power penalty at a bit error rate of $1e^{-9}$ (measured after the VOA) and the reverse

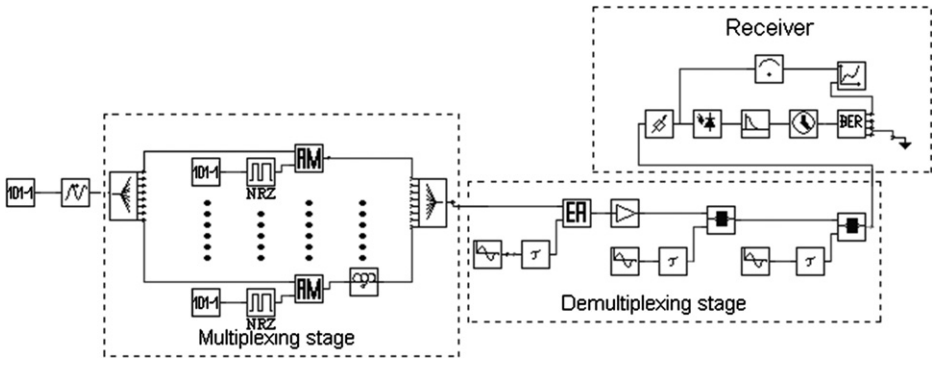

Fig. 7. Simulation model of 80 Gb/s OTDM system using VPI software package.

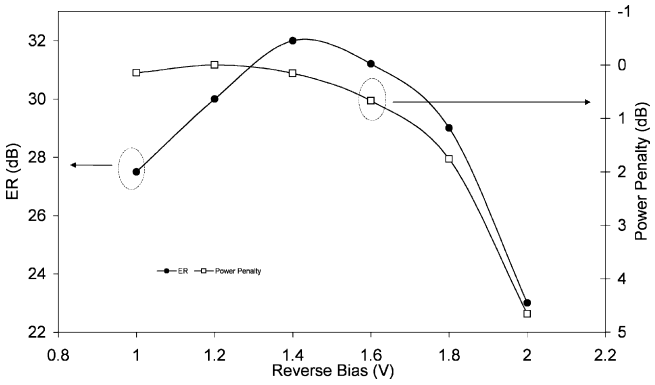

Fig. 8. Extinction ratio and BER performance at $1e^{-9}$ as a function of reverse bias, measured from a VPI model.

bias condition of the EAM. Fig. 8 illustrates the ER and BER performance as a function of reverse bias.

An excellent correlation is observed between the simulation and experimental results. The extinction ratio (ER) measured using the FROG technique shows good agreement with the simulation results. Again, as with the experiment, an optimum ER is realized at a reverse bias of 1.4 V and then falls off rapidly. This ER fall off is again due to the steepness of the transmission profile of the EAM and shows discrepancies of less than 1 dB in comparison to the experiment, which is in excellent agreement. The BER performance at a series of bias conditions shows the same trend as that experienced in the experiment. There is a slightly smaller power penalty of 4.8 dB experienced in the simulation model. The power penalty does not fall off as rapidly in the modeled system due to a more ideal receiver than that used in the experiment which suffers from a lower noise level, thus reducing the power penalty measured at $1e^{-9}$. As in the experiment the optimum BER performance is realized at a reverse bias of 1.2 V.

6. Conclusion

We have demonstrated the complete characterization of an electro-absorption modulator over a wide range of RF drive voltages and reverse bias conditions for pulse generation and optical demultiplexing applications. The Frequency Resolved Optical Gating (FROG) technique was employed to create a complete performance map for the EAM in terms of pulse width (PW), frequency chirp and extinction ratio (ER). The EAM generated pulses with a varying FWHM between 9 and 4 ps, and with an extinction ratio varying from 22 to 33 dB. The frequency chirp (measured in GHz/ps) also varied with respect to the EAM's reverse bias from about 7 to 0 GHz/ps. By compiling this performance map we are able to tailor the generated pulses for use in high-speed optical systems.

The EAM is also utilized as a demultiplexing component in an 80 Gb/s OTDM system and its performance was monitored over a range of bias conditions. A power penalty of 5.5 dB was experienced at a reverse bias of 2 V. This penalty was the result of the gates varying ER and a changing signal to noise ratio (SNR) due to the gradient of the EAM's transfer characteristic. Finally, the experimental results were verified using a simulation model which exhibited excellent correlation. This result demonstrates how the FROG measurement technique may be used for optimizing both transmitters and receivers (demultiplexers) for high speed OTDM systems.

References

[1] R. Ludwig, U. Feiste, E. Dietrich, H.G. Weber, D. Breuer, M. Martin, F. Kuppers, Electron. Lett. 35 (1999) 2216.
[2] B. Konrad, K. Petermann, J. Berger, R. Ludwig, C.M. Weinert, H.G. Weber, B. Schmauss, J. Lightwave Technol. 20 (2002) 2129.
[3] J. Debeau, B. Kowalski, R. Boittin, Opt. Lett. 23 (2000) 1784.
[4] D.G. Moodie, M.J. Guy, M.J. Harlow, A.D. Ellis, C.W. Ford, S.D. Perrin, in: IEE Colloquium on High Speed and Long Distance Optical Transmission, April 1996, p. 5/1.
[5] P.L. Mason, A. Wonfor, D.D. Marcenac, D.G. Moodie, M.C. Brierley, R.V. Penty, I.H. White, S. Bouchoule, in: Proc. LEOS 1997, vol. 1, November 1997, Paper TuS2, p. 289.
[6] P. Anandarajah, M. Rensing, L.P. Barry, OSA Appl. Opt. 44 (2005) 7867.
[7] H.F. Chou, Y.J. Chiu, J.E. Bowers, in: Proc. CLEO 2002, Paper CMI 1.
[8] J. Yu, K. Kojima, N. Chand, in: Proc. LEOS 2001, November 2001, Paper TuBB4.
[9] H.F. Chou, J.E. Bowers, D.J. Blumenthal, IEEE Photon. Technol. Lett. 16 (2004) 1564.
[10] D.D. Marcenac, A.D. Ellis, D.G. Moodie, Electron. Lett. 34 (1998) 101.
[11] T. Ohno, S. Kodama, T. Yoshimatsu, K. Yoshino, H. Ito, Electron. Lett. 40 (2004) 1285.
[12] R. Trebino, K.W. DeLong, D.N. Fittinghoff, J.N. Sweerser, M.A. Krumbugel, B.A. Richman, Rev. Sci. Instrum. 68 (1997) 3277.
[13] R. Trebino, Frequency-Resolved Optical Gating: The Measurement of Ultrashort Laser Pulses, Kluwer Academic Publishers, 2000.
[14] A.M. Clarke, P.M. Anandarajah, L. Bramerie, C. Giugnard, D. Massoubre, A. Shen, J.L. Oudar, L.P. Barry, J.C. Simon, in: Proc. ECOC 2006, Paper Th1.4.6.
[15] A.M. Clarke, P.M. Anandarajah, L. Bramerie, C. Giugnard, R. Maher, D. Massoubre, A. Shen, J.L. Oudar, L.P. Barry, J.C. Simon, IEEE Photon. Technol. Lett. (2007), in press.
[16] A.M. Clarke, M.J. Connelly, P. Anandarajah, L.P. Barry, D. Reid, IEEE Photon. Technol. Lett. 17 (9) (2005).
[17] M.J. Connelly, A.M. Clarke, P. Anandarajah, L.P. Barry, in: Proc. Numerical Simulation of Optoelectronic Devices, NUSOD 2005, September 2005, p. 129.